Supporting Information

Local Water Content in Polymer Gels Measured With Super-Resolved Fluorescence Lifetime Imaging

Sankar Jana,[a] Oleksii Nevskyi,[b] Hannah Höche,[a] Leon Trottenberg,[a] Eric Siemes,[a] Jörg Enderlein,[b,c] Alexandre Fürstenberg,[d] Dominik Wöll.*[a]

[a] *Institute of Physical Chemistry, RWTH Aachen University, Landoltweg 2, 52074 Aachen, Germany. Tel: +49 241 80 98624; E-mail: woell@pc.rwth-aachen.de*

[b] *Third Institute of Physics - Biophysics, Georg August University, Göttingen, Germany.*

[c] *Cluster of Excellence "Multiscale Bioimaging: from Molecular Machines to Networks of Excitable Cells" (MBExC), Georg August University, 37077 Göttingen, Germany.*

[d] *Department of Physical Chemistry and Department of Inorganic and Analytical Chemistry, University of Geneva, 1211 Geneva, Switzerland.*

Contents

1 Synthesis and labeling of PNIPAM-co-APMH microgels **2**

2 Dynamic Light Scattering (DLS) measurements **2**

3 Microgel sample preparation **3**

4 Fluorescence Lifetime Imaging (FLIM) microscopy **3**

5 Data processing and reconstruction of super resolved-FLIM (FL-SMLM) Image **4**

6 Microgel data analysis and clustering **4**

7 FLIM images and fluorescence lifetime distributions **4**

8 Stern-Volmer analysis **9**

9 Radial localization density and lifetime distributions **10**

1 Synthesis and labeling of PNIPAM-co-APMH microgels

N-isopropylacrylamide (NIPAM, 97 %, AcrosOrganics), *N,N'*-methylenediacrylamide (BIS, 98 %, AppliChem), *N*-(3-aminopropyl)methacrylamide hydrochloride (APMH, 98 %, Sigma), cetyltrimethylammoniumbromide (CTAB, AppliChem) and initiator 2,2'-azobis(2-amidinopropane)dihydrochloride (V50, 97 %, Sigma) and fluorescent dye ATTO 655 NHS-ester (ATTO-TEC GmbH) were used as received without further purification. Polymerization was performed in a 250 mL three-necked round-bottom flask, equipped with a reflux condenser, overhead stirrer, thermometer, and nitrogen inlet. The initial total monomer concentration was kept constant at 250 mM. 4.544 g NIPAM (40.2 mmol, 93 mol %), 122.8 mg APMH (0.86 mmol, 2 mol %) and 332.9 mg BIS (2.16 mmol, 5 mol %) were dissolved in 168 mL water. The oil-bath was then heated up to 70 °C. The sealed apparatus was thoroughly flushed with nitrogen at least 1 h prior to initiation. Before free radical polymerization was initiated the nitrogen inlet was drawn out of the liquid phase to avoid foaming and 2.4 mg cetyltrimethylammoniumbromide (CTAB) (0.05 × cmc, where cmc is the critical micellization concentration) dissolved in 2 mL degassed water was added. After initiation with 46.7 mg V50 (1 mM in the batch) dissolved in 2.7 mL degassed water, the initially transparent solution became progressively turbid. The mixture was allowed to react for a period of 5 h in the presence of nitrogen under stirring at a speed of 500 min^{-1}. To eliminate possible chemical residues, especially to remove the surfactant, the microgel dispersion was purified by ultracentrifugation (Beckman Coulter, Optima™ XPN) three times (30.000 min^{-1}, respective 21.000 × *G* for 1 h, where *G* is the gravity constant). For each cycle the supernatant was removed and the microgels redispersed in double distilled water. The dynamic light scattering (DLS) data for different temperatures are presented in Fig. S1. Covalent labeling of PNIPAM-co-APMH microgels via NHS-ester reaction (see also Scheme S1): For fluorescent labeling, 30 mg of the dried microgel powder was redispersed in 15 mL of water. The pH of the redispersed microgel solution was adjusted to a slightly basic value (pH 8) using 0.1 M NaOH solution to avoid undesired hydrolysis reactions. 10 µL of a 4 mM ATTO 655-NHS ester in DMSO (in stoichiometric excess) was added at room temperature and allowed to react for 24 h. Unbound dye was removed again by ultracentrifugation as described above.

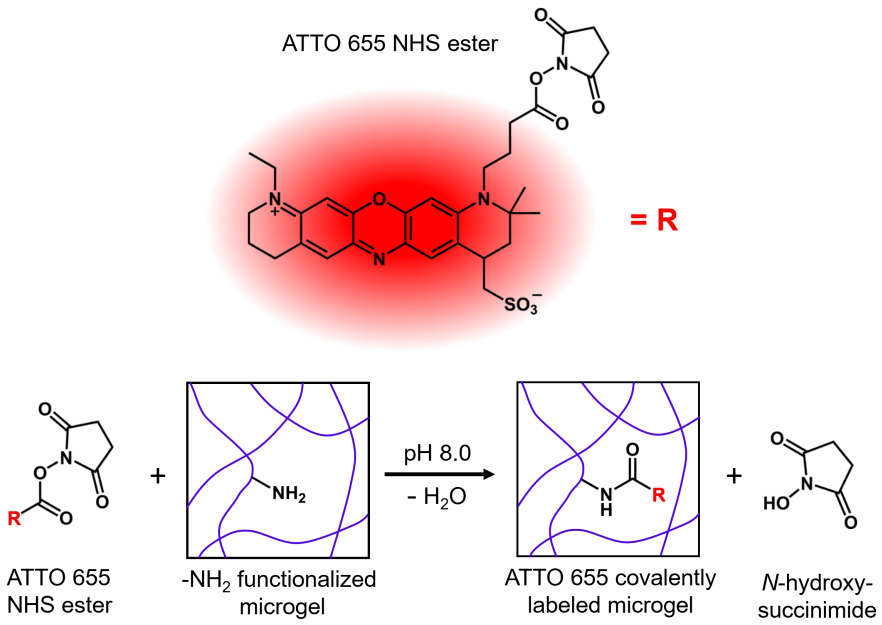

Scheme S1 Top: Chemical structure of ATTO 655 NHS ester; bottom: reaction scheme for covalent labeling of $-NH_2$ functionalized microgels with ATTO 655 NHS ester.

2 Dynamic Light Scattering (DLS) measurements

DLS measurements were performed on an ALV setup equipped with a 633 nm HeNe laser (JDS Uniphase, 35 mW), a goniometer (ALV, CGS-8F), digital hardware correlator (ALV 5000), two avalanche photo diodes (Perkin Elmer, SPCM-CD2969), a light scattering electronics (ALV, LSE-5003), an external programmable thermostat (Julabo F32) and a bath filled with toluene to match the refractive index of the sample container. The temperature was measured inside the bath and regarded as sample temperature. The PNIPAM-*co*-APMH microgels sample was highly diluted with HPLC-

grade water to avoid multiple scattering and was measured at a fixed scattering angle of 90°. Temperature-dependent measurements were performed in the range of 20 °C to 50 °C in 2 °C steps. The intensity time correlation functions were analyzed according to the methods of cumulants. The cumulants k_1 from a second order cumulant fit were plotted against q^2. The data were fitted with a homogeneous linear regression where the slope equals the diffusion coefficient D. The Stokes-Einstein equation was used to calculate the hydrodynamic radius r_H from the diffusion coefficient.

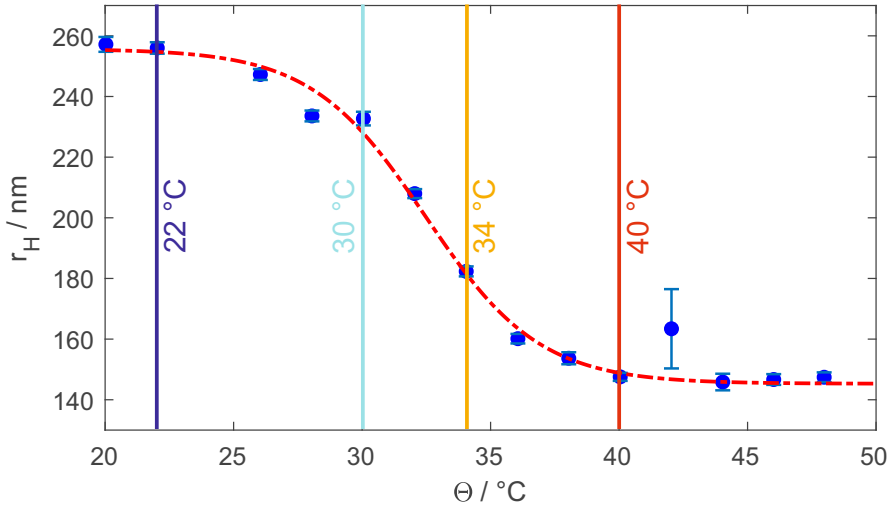

Figure S1 Temperature-dependent DLS data of the microgels investigated. The dashed line presents a fit to the experimental data with the sigmoidal function $\frac{\Delta r}{1+\exp\left(-b\cdot(\Theta-\Theta_{\mathrm{VPTT}})\right)}+r_{\mathrm{collapsed}}$ with $\Delta r = 110.4$ nm, $b = -0.45$ °C^{-1}, $\Theta_{\mathrm{VPTT}} = 32.5$ °C, and $r_{\mathrm{collapsed}} = 145.3$ nm. The temperatures that were chosen for our FL-SMLM measurements are indicated with vertical lines in the color code also used in Figure 3 of the main paper.

3 Microgel sample preparation

The ATTO 655-labeled microgel sample was resuspended in pure H_2O and pure D_2O medium, respectively, to prepare the stock samples which were used further to prepare the diluted samples using water with different H_2O:D_2O ratios. The dilute microgel samples were spin-coated on a Hellmanex III-washed, plasma-cleaned coverslip. After spin coating, the coverslip was washed three times with freshly prepared 5 mM cysteamine solution (the same as used below as blinking agent), and then placed into a BioCell (BioCell for AFM, Bruker). The BioCell is a coverslip-based fluid cell that is used for temperature-dependent fluorescence measurements. The BioCell was filled with 1 mL of a freshly prepared solution containing 5 mM cysteamine as blinking agent and covered with another coverslip from the top.

4 Fluorescence Lifetime Imaging (FLIM) microscopy

FLIM measurements were performed on a PicoQuant Microtime 200 system (PicoQuant, GmbH, Berlin, Germany) equipped with a FLIMbee galvanometric scanner and an inverted microscope (IX83, Olympus). A pulsed NKT continuum laser with 20 MHz repetition rate, SuperK EVO (NKT Photonics), was used as the excitation source. A spectral window between 630 nm and 640 nm was chosen with a SuperK VARIA tunable filter. The laser power entering the microscope was 1.2 mW. A Chroma ZT633RDC-UF3 flat dichroic mirror from Chroma, ZT633RDC-UF3 was used to direct the excitation light into the microscope and through the FLIMbee scanner. A 60× water immersion objective lens with NA 1.2 (UPLSAPO60XW, Olympus, Japan) was used to focus on the sample. The sample position can be adjusted by using a manual XY stage (JPK MotorStage Olympus) and a z-piezo stage (Nano-ZL100, MadCityLabs). Fluorescence from the sample was collected by the same objective and went through the FLIMbee scanner and through the dichroic mirror. The excitation laser light was blocked in the emission path by a long-pass filter (ET655LP, Chroma).

The beam was then focused onto the pinhole (100 μm P100S, Thorlabs) using an achromatic tube lens (TTL180-A, Thorlabs). The emitted light was then collimated by a 100 mm focal length lens. A 685/75 BrightLine HC bandpass filter, Semrock, was used immediately in front of the lens. Finally, the emission light was focused on a SPAD detector

(SPCM-AQRH, Excelitas) with an achromatic lens.

The output signal of the photon detector was recorded by a TCSPC system (HydraHarp 400, PicoQuant) synchronized with the trigger signal of the excitation laser. The measurements were acquired using software (SymPhoTime 64, PicoQuant) that controlled both the TCSPC system and the scanner system. Typically, a $10 \times 10\,\mu m^2$ region of the sample was scanned with a pixel size of 100 nm, a dwell time of $2.5\,\mu s$/pixel and a frame rate of 20 Hz. 80000 frames were acquired. For the temperature-dependent measurements, the BioAFM system with the BioCell for AFM of Bruker was used, which is a coverslip based fluid cell for single-molecule fluorescence with temperature control. The system has a temperature resolution of $0.1\,^{\circ}C$ with a temperature range of 15 to $60\,^{\circ}C$. Actual data were recorded after two hours of temperature equilibration of the sample.

5 Data processing and reconstruction of super resolved-FLIM (FL-SMLM) Image

FLIM data analysis, FL-SMLM image reconstruction, and visualization were performed using the free Matlab-based framework TrackNTrace available on the open access platform GitHub (`https://github.com/scstein/TrackNTrace`). From the raw scan data, 10 frames were binned to obtain a sufficient number of photons per localization event. Signal detection and refinement process were carried out with the cross correlation and TNT Fitter plugins, respectively, using default parameters as given in TrackNTrace. Single emitter tracking was performed using the TNT Nearest Neighbor algorithm with 1 as the minimum track length, maximum tracking radius, and no gap closing. The fit lifetime algorithm was used for lifetime fitting. Each localization position was refitted in a sum image of each frame of the track using a Gaussian maximum likelihood estimator (MLE) fit. To extract TCSPC traces, a mask radius of two and summation over all frames within the track was chosen. All localizations consisting of more than 100 photons were considered, and the corresponding TCSPC time traces were fitted (with a maximum of 5 trials) using the MLE monoexponential tail fit with a cutoff of 0.3 ns and in a lifetime range of 0.5 to 5 ns. During post-processing and before reconstruction of the final FL-SMLM image, the localizations were filtered according to the quality of the lifetime fit χ^2 between 0.9 and 1.1. In addition, drift correction was performed using the Redundant Cross-Correlation (RCC) method. The FL-SMLM images were calculated as a Gaussian weighted average of all localizations.

6 Microgel data analysis and clustering

The analysis of the output data from TrackNTrace was performed using MATLAB and a Python-based workflow. In the first step of this workflow, the localization data were clustered using a MATLAB application based on the Python implementation of the HDBSCAN data clustering algorithm. The input parameters for the clustering algorithm were user-defined in order to obtain well-separated clusters. It was then assumed that each extracted cluster corresponds to a single microgel. Therefore, clusters containing multiple ill-separated microgels were excluded from further analysis. Due to the spherical symmetry of the microgels used the center of each microgel can be approximated by the median of all localizations in a cluster. For further analysis, the absolute coordinates of the localizations in each cluster were converted to relative coordinates from the center and the Euclidean distance of each localization to the corresponding center was calculated. In the next step, the localization density was calculated. All relative localizations corresponding to the same measurement conditions were summed and binned based on the distance from the center. The bins were chosen so that the area of the annular bins remained the same for all bins. The number of localizations in each bin was then normalized by the area of the bins and the total number of localizations to allow comparison between different measurements.

7 FLIM images and fluorescence lifetime distributions

In the following, the complete series of measured FLIM images and fluorescence lifetime distributions at $22\,^{\circ}C$ and at $40\,^{\circ}C$ are presented in Figures S2 and S3. Furthermore, the normalized radial localization densities at both temperatures and different H_2O–D_2O solvent mixtures are shown in Figure S4.

For reference and comparison with the FL-SMLM images presented above, we also measured confocal FLIM images of spin-coated microgels in the dry state and after the addition of water in the swollen state at $22\,^{\circ}C$. Note that FL-

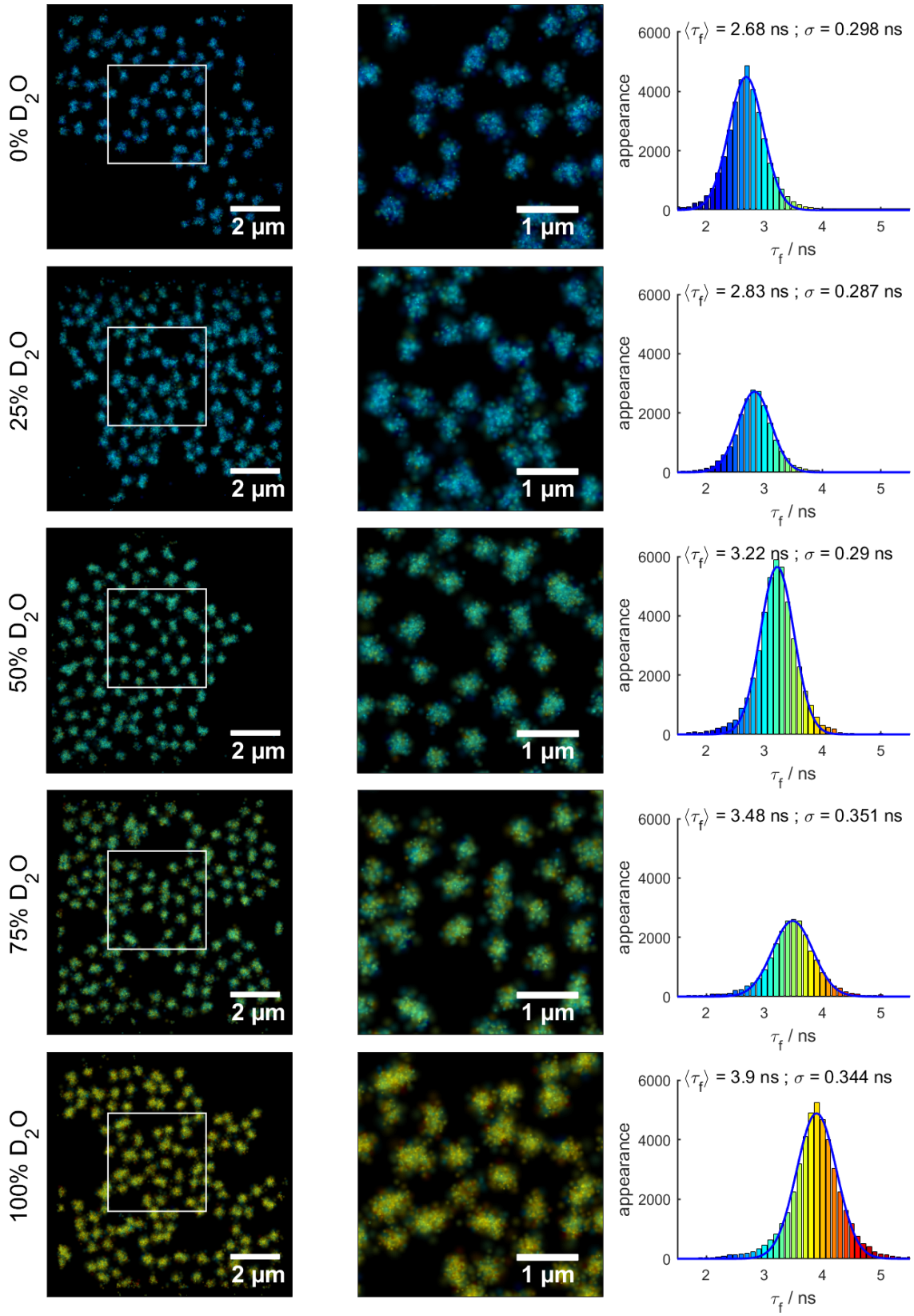

Figure S2 FL-SMLM images (1st and 2nd column) and corresponding fluorescence lifetime distributions (3rd column) for microgels at 22 °C in different H_2O/D_2O-ratios. The selected region within the FL-SMLM image in 1st column indicated by the white square is zoom-in and shown in 2nd column. From top to bottom, data of measurements in 0 % D_2O, in 25 % D_2O, in 50 % D_2O, in 75 % D_2O, and m-o in 100 % D_2O, respectively, are presented. The FL-SMLM images are intensity-weighted lifetime distributions color-coded in the corresponding fluorescence lifetime. Each point cloud represents a microgel. The same color code is used for the fluorescence lifetime distribution histograms. The average fluorescence lifetimes $\langle \tau_f \rangle$ as obtained by Gaussian fits and their widths σ are also noted.

SMLM is not possible for our system in the dry state since we cannot add switching agent. The laser power entering the microscope was 15 μW. For the FLIM images, 500 frames were recorded and binned into a single image. All other conditions remained the same as described in section 4. We assume that most water molecules inside microgels are removed during spin coating resulting in dry microgels as it is indicated by the measured fluorescence lifetime. As presented in Figure S5(top), the average fluorescence lifetime is 3.82 ns which is very similar to the lifeftime of our FL-SMLM measurements in pure D_2O indicating that no significant amount of water was left. After the addition of a drop of water, the dry microgels reswell again. As shown in Figure S5(bottom), the distribution became at least bimodel and the average fluorescence lifetime $\langle \tau_f \rangle$ of the signal between 1.5 and 3 ns dropped to a value 2.57 ns which is close to the value of 2.68 ns in Figure S2 (upper row). We observed a tail at higher fluorescence lifetimes (between 3 and 4 ns) indicating that the microgels were not fully swollen anymore which could indicate that the time of approximately 2 h between the addition of water and the measurement was caused some irreversible change of conformation due to the adhesion to the surface. The investigation of this interesting behavior is beyond the scope of our current work, but we plan to have a deeper look into that in the future. It should be also noted that due to the attachment at the surface no significant swelling in lateral dimensions was observed.

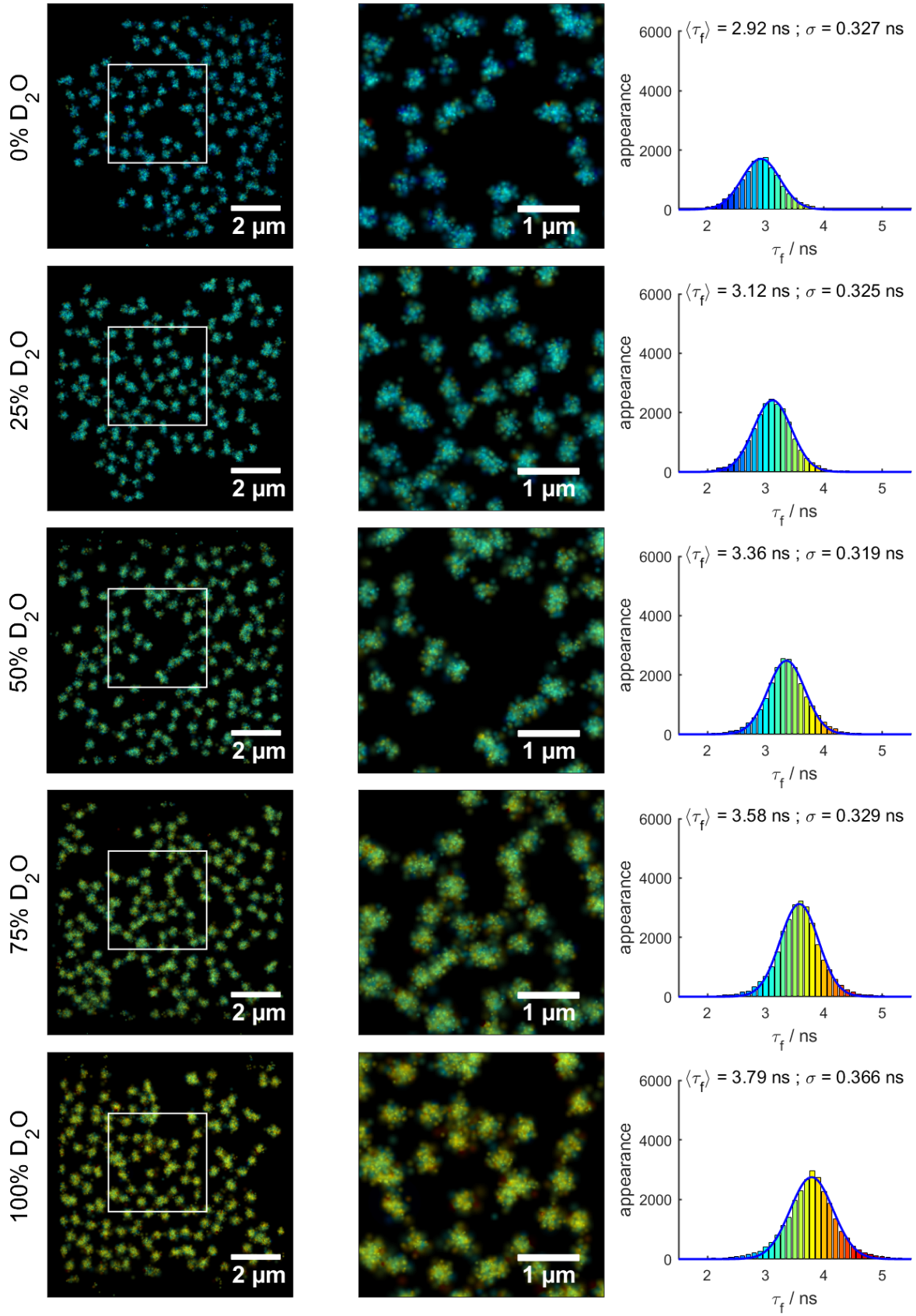

Figure S3 FL-SMLM images (1^{st} and 2^{nd} column) and corresponding fluorescence lifetime distributions (3^{rd} column) for microgels at $40\,^{\circ}\mathrm{C}$ in different H_2O/D_2O-ratios. The selected region within the FL-SMLM image in 1^{st} column indicated by the white square is zoom-in and shown in 2^{nd} column. From top to bottom, data of measurements in $0\,\%$ D_2O, in $25\,\%$ D_2O, in $50\,\%$ D_2O, in $75\,\%$ D_2O, and m-o in $100\,\%$ D_2O, respectively, are presented. The FL-SMLM images are intensity-weighted lifetime distributions color-coded in the corresponding fluorescence lifetime. Each point cloud represents a microgel. The same color code is used for the fluorescence lifetime distribution histograms. The average fluorescence lifetimes $\langle \tau_f \rangle$ as obtained by Gaussian fits and their widths σ are also noted.

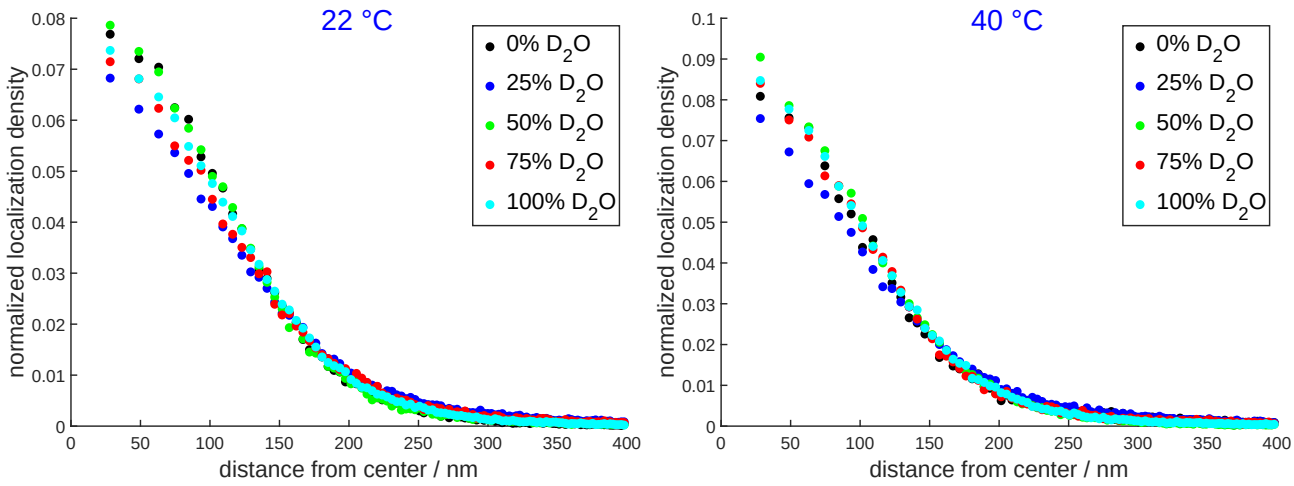

Figure S4 Radial distribution of ATTO 655 localizations within microgels in different H_2O–D_2O solvent mixtures at 22 °C and at 40 °C, respectively.

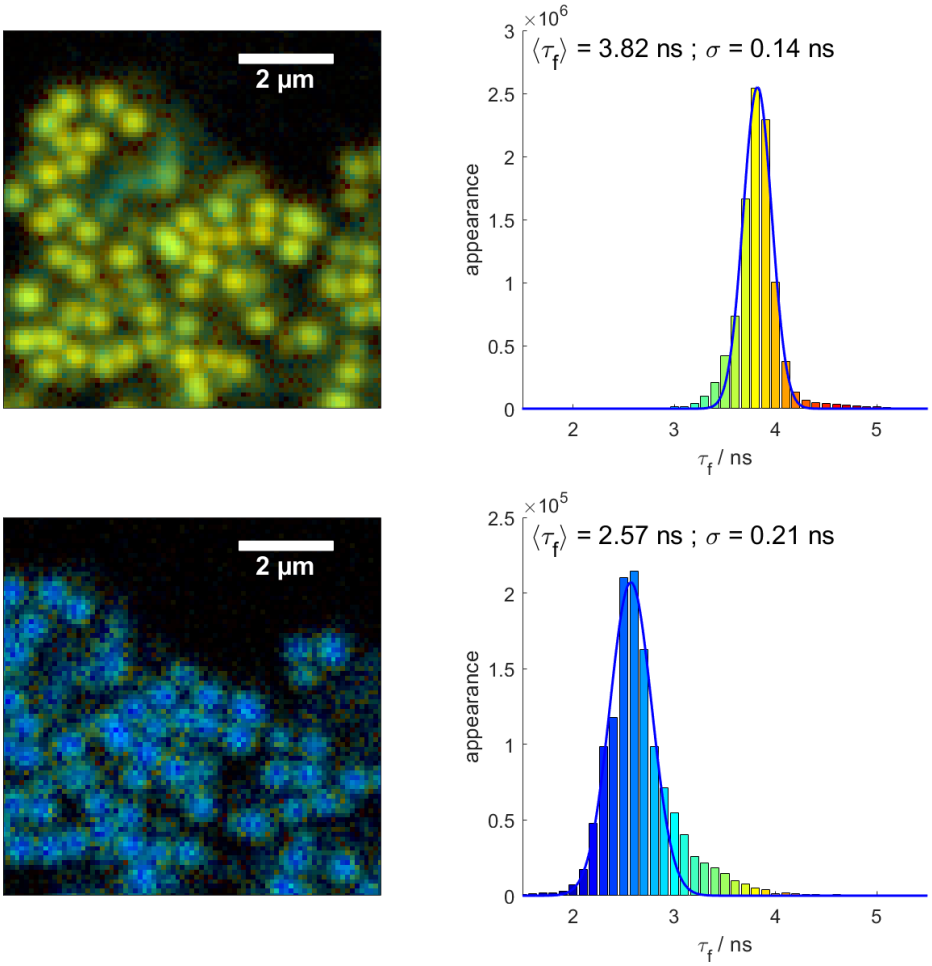

Figure S5 Confocal FLIM images (left column) and corresponding lifetime histograms (right column) of ATTO 655-labeled NIPAM-co-APMH microgels at 22 °C; Top: in the dry state; microgels were spin-coated onto plasma-cleaned glass coverslip. Bottom: in the swollen state after the addition of water to the dry sample. Shown left are the fluorescence lifetime images and right the corresponding distributions with Gaussian fits. Note that for the wet state, the data between 1.5 and 3 ns were chosen for the fit since the tail between 3 and 4 ns seems to be caused by the microgel partially being collapsed at the surface.

8 Stern-Volmer analysis

The Stern-Volmer analysis used in the paper will be outlined in the following paragraph. Starting from the well-known Stern-Volmer equation

$$\frac{\tau_{f,0}}{\tau_f} = 1 + k_q \cdot \tau_{f,0} \cdot c_{\mathrm{H_2O},loc} \tag{1}$$

with the fluorescence lifetimes τ_f and $\tau_{f,0}$ where the latter is obtained without H_2O as a quencher, the quenching constant k_q, and the local concentration $c_{\mathrm{H_2O},loc}$ of H_2O around the fluorophore. If the fluorophore is in pure H_2O, its fluorescence will be maximally quenched. Otherwise the effective quenching will be determined by the local amount of H_2O around the fluorophore. Two possibilities in our system to substitute H_2O molecules around the fluorophore are either by the polymer network of the microgel to which the dye is covalently linked or by D_2O, if added to the solvent mixture. Defining $c_{\mathrm{H_2O},0}$ as the concentration of water molecules in pure H_2O, $x_{\mathrm{H_2O}}$ as the fraction of H_2O in the (added / external) H_2O–D_2O solvent mixture and $f_{q,loc}$ as the local water content around the dye with respect to the one in pure water solvent, which also describes the local accessibility of water to the dye, we can transform the equation as follows:

$$\frac{\tau_{f,0}}{\tau_f} = 1 + k_q \cdot \tau_{f,0} \cdot c_{\mathrm{H_2O},0} \cdot f_{q,loc} \cdot x_{\mathrm{H_2O}} \tag{2}$$

It should be noted that the product $k_q \cdot c_{\mathrm{H_2O},0}$ equals the quantity k_s and that $f_{q,loc}$ equals the quantity f_q of the paper of Maillard *et al.* [1]. k_s is the maximal quenching rate constant observed for the dye in pure H_2O. $f_{q,loc}$ can be interpreted as the number of water molecules accessible to the dye with respect to the maximal number of accessible water molecules in pure water as the solvent:

$$f_{q,loc} = \frac{N_{water,loc}}{N_{water,loc,max}} \tag{3}$$

It should be noted that we neglected the differences in density of H_2O and D_2O, here. Consequently, our hypothesis is that the space not filled with water molecules is occupied by polymer. Thus, the fraction of water molecules $f_{q,loc}$ around the fluorophore can be determined from the slope of the Stern-Volmer plot of $\frac{\tau_{f,0}}{\tau_f}$ against $x_{\mathrm{H_2O}}$ since the constants k_q, $\tau_{f,0}$ and $c_{\mathrm{H_2O},0}$ can be measured or are known, respectively.

As reference for the Stern-Volmer plots presented in the main paper, we performed the corresponding experiments with free ATTO 655 where we changed the H_2O content. Increasing the H_2O concentration resulted in a reduction of the fluorescence lifetime which can be fitted well with a linear function in the Stern-Volmer plot. As shown in S6, the Stern-Volmer plots are very similar at both temperatures addressed in our work.

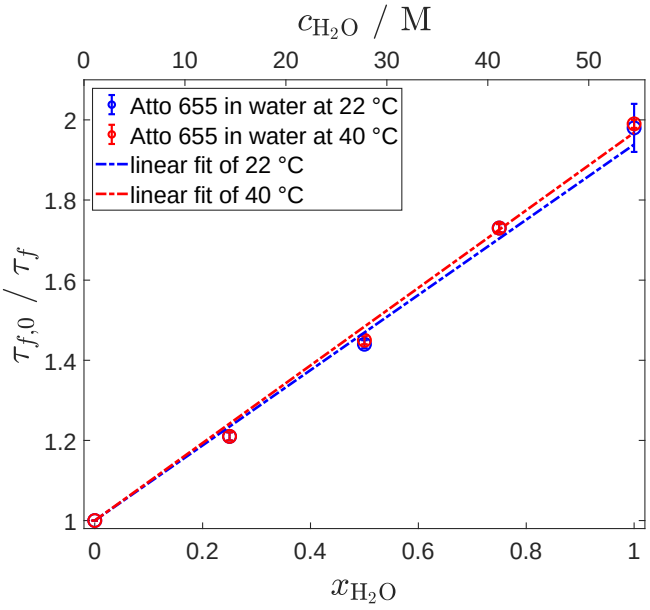

Figure S6 Stern-Volmer plot for fluorescence quenching of free ATTO 655 by surrounding H_2O molecules at 22 °C and at 40 °C. The ratio of the fluorescence lifetimes in pure D_2O $\tau_{f,0}$ and the fluorescence lifetime τ_f at the respective H_2O–D_2O solvent mixture is plotted against the molar concentration of water. The data at 22 °C are presented in blue, and the ones at 40 °C are shown in red. The dashed lines are linear fits with a fixed value of 1 at $[H_2O] = 0$.

9 Radial localization density and lifetime distributions

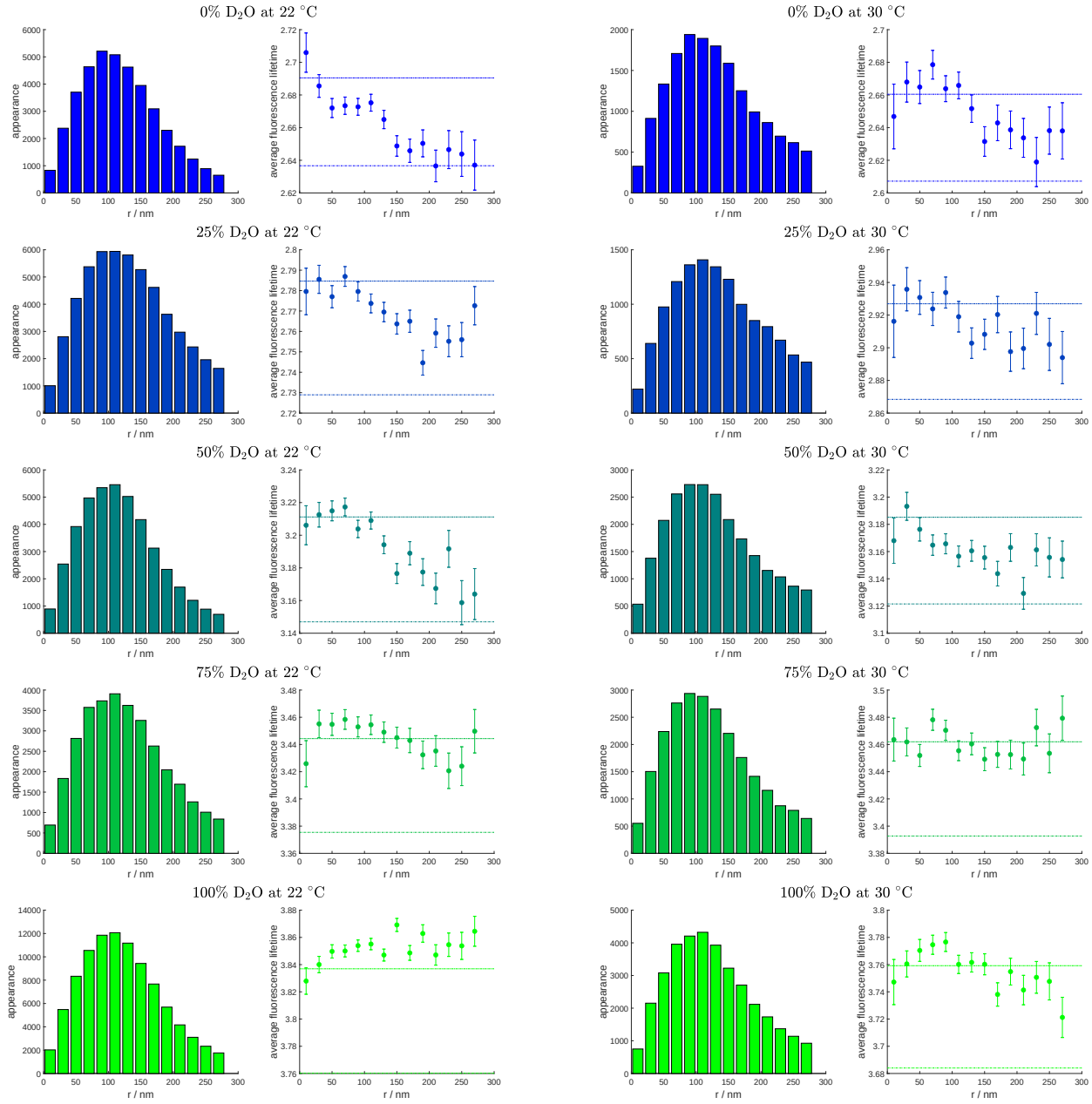

Figure S7 Radial localization density and lifetime distributions at 22 °C(left) and at 30 °C for different H_2O/D_2O-ratios from top to bottom 0 %, 25 %, 50 %, 75 %, and 100 % D_2O, respectively. The upper dashed line presents the average lifetime of all localization between $r = 0$ and $r = 40$ nm, and the lower dashed dotted line presents 98 % of this lifetime. Both lines serve as guide to the eyes.

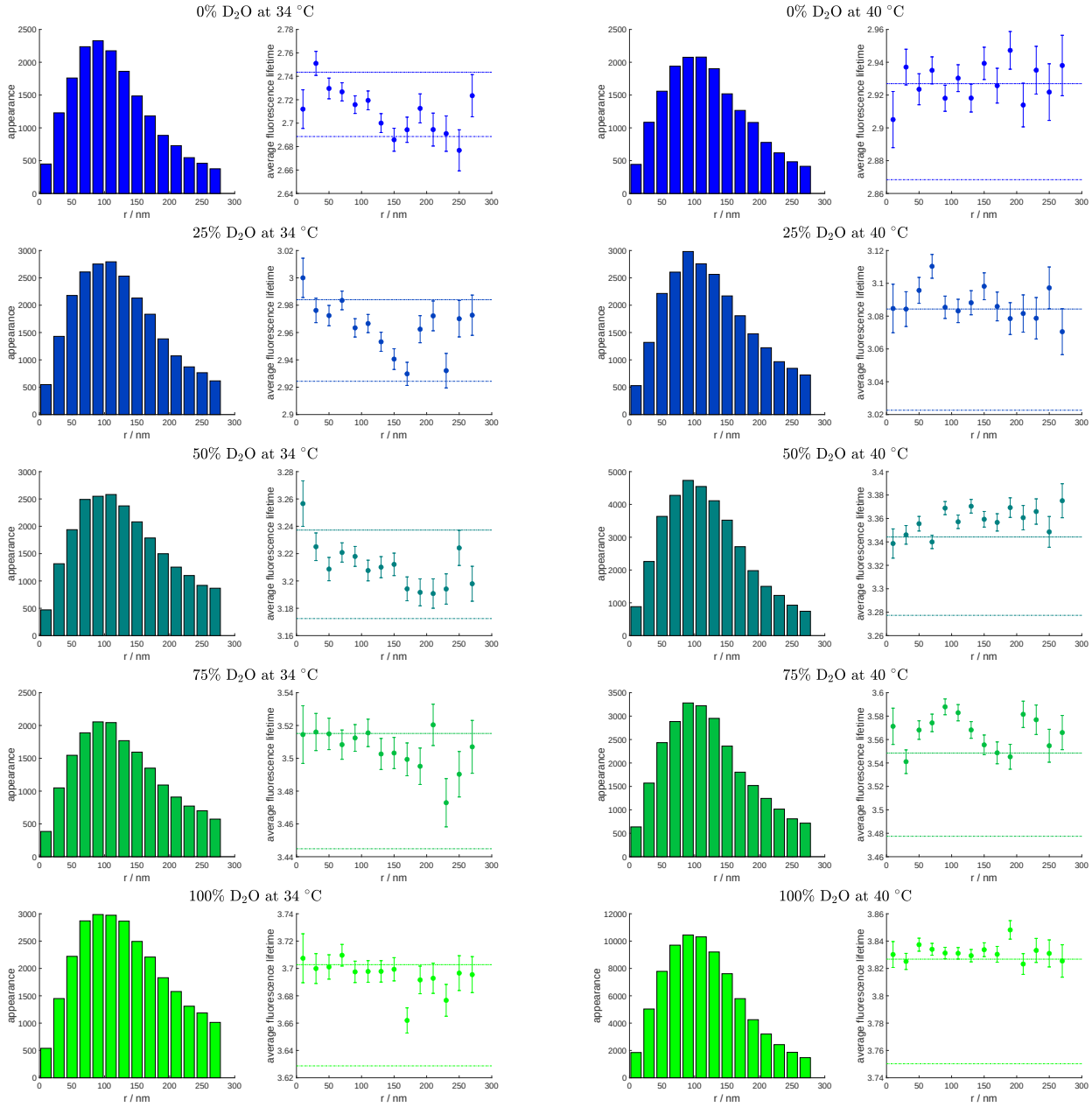

Figure S8 Radial localization density and lifetime distributions at 34 °C(left) and at 40 °C for different H_2O/D_2O-ratios from top to bottom 0 %, 25 %, 50 %, 75 %, and 100 % D_2O, respectively. The upper dashed line presents the average lifetime of all localization between $r = 0$ and $r = 40$ nm, and the lower dashed dotted line presents 98 % of this lifetime. Both lines serve as guide to the eyes.

Notes and references

1 J. Maillard, K. Klehs, C. Rumble, E. Vauthey, M. Heilemann, A. Fürstenberg, *Chem. Sci.* **2021**, *12*, 1352.